The European Zoological Journal

ISSN: (Print) 2475-0263 (Online) Journal homepage: http://www.tandfonline.com/loi/tizo21

Effects of X-ray irradiation on haemocytes of Procambarus clarkii (Arthropoda: Decapoda) males

A. Giglio, C. Manfrin, M. Zanetti, L. Aquiloni, E. Simeon, M. K. Bravin, S. Battistella & P. G. Giulianini

To cite this article: A. Giglio, C. Manfrin, M. Zanetti, L. Aquiloni, E. Simeon, M. K. Bravin, S. Battistella & P. G. Giulianini (2018) Effects of X-ray irradiation on haemocytes of Procambarus clarkii (Arthropoda: Decapoda) males, The European Zoological Journal, 85:1, 26-35, DOI: 10.1080/24750263.2017.1423119

To link to this article: https://doi.org/10.1080/24750263.2017.1423119

© 2018 The Author(s). Published by Informa UK Limited, trading as Taylor & Francis Group.

Published online: 22 Jan 2018.

Submit your article to this journal

Article views: 37

View related articles

View Crossmark data

Full Terms & Conditions of access and use can be found at
http://www.tandfonline.com/action/journalInformation?journalCode=tizo21

The European Zoological Journal, 2018, 26–35
Vol. 85, No. 1, https://doi.org/10.1080/24750263.2017.1423119

Taylor & Francis
Taylor & Francis Group

Check for updates

Effects of X-ray irradiation on haemocytes of *Procambarus clarkii* (Arthropoda: Decapoda) males

A. GIGLIO[1], C. MANFRIN[*2], M. ZANETTI[3], L. AQUILONI[4], E. SIMEON[2], M. K. BRAVIN[2], S. BATTISTELLA[2], & P. G. GIULIANINI[2]

[1]*Department of Biology, Ecology and Earth Sciences, University of Calabria, Rende, Italy,* [2]*Department of Life Sciences, University of Trieste, Trieste, Italy,* [3]*Ente Tutela Pesca del Friuli Venezia Giulia, Udine, Italy, and* [4]*Itinera C.E.R.T.A. scrl, Montevarchi, Arezzo, Italy*

(Received 29 September 2017; accepted 20 December 2017)

Abstract

The red swamp crayfish *Procambarus clarkii* is an invasive alien species spreading worldwide. The sterile male release technique (SMRT) is among the methods used to contrast the growth of *P. clarkii* populations within invaded areas. In this study males underwent X-ray sterilisation with a dose of 40 Gy and their immunocompetence was analysed in comparison to untreated animals to ascertain whether radiation can affect welfare parameters other than reproductive organs. The present research investigated the immune function in *P. clarkii* males in term of (1) morphological haemocyte characterisation by transmission electron microscopy to identify the main phagocyting haemocyte after *in vivo* artificial non-self challenge with latex beads; (2) total and differential haemocyte counts; and (3) basal and total phenoloxidase activities as components of the humoral defence. Three types of circulating haemocytes were characterised via transmission electron microscopy: hyaline, semigranular and granular haemocytes. The ultrastructural features of haemocyte granules allowed the characterisation of a fourth type of haemocyte, the medium granule haemocyte. *In vivo* artificial non-self-challenge with latex beads identified the semigranular haemocytes as primarily involved in phagocyting activity. Circulating haemocytes of males irradiated with a dose of 40 Gy, after 20 days, showed a significantly lower diameter in the granules of hyaline and semigranular haemocytes, but no other evident ultrastructural alterations in comparison with un-irradiated animals were found. Irradiated males showed a significant decrease of about 80% of circulating haemocytes and an increase in frequency of semigranular and granular haemocytes. No significant differences in basal and total phenoloxidase activity were recorded and this could, in part, explain the good survival level of irradiated males despite the drastic decline of the haemocyte number. This study represents the basis to appraise whether SMRT affects important functions, such as those of the immune system, in addition to altering the gonad tissue.

Keywords: Procambarus clarkii, *irradiation, males, haemocytes, X-ray*

Introduction

Procambarus clarkii (Girard, 1852) is an invasive alien species spread worldwide with significant economic and ecologic impact. For this reason, a wide number of previous studies have investigated its life cycle, physiology and reproductive behaviour to limit its diffusion in freshwater environments (Aquiloni & Gherardi 2010; Peruzza et al. 2015; Souty-Grosset et al. 2016; Yazicioglu et al. 2016). The sterile male release technique (SMRT) has been chosen in Friuli Venezia Giulia region (Italy) as part of the strategy to control the red swamp crayfish local populations. The SMRT consists in the release into the environment of sterile males that are sexually active and able to compete with untreated males for mating partners. For SMRT, it is thus mandatory that treated animals lack physiological and behavioural damages leading to suppression of competitiveness towards wild individuals. Recently, the gonad damage induced by ionising radiation was described in *P. clarkii* males (Piazza et al. 2015), but no data are available on their welfare. Immunocompetence has been chosen to assess the status of health of males after radiation. To evaluate the immune function in *P. clarkii*, the following parameters were considered: (1) morphology of haemocytes, as characterised by transmission electron microscopy, and to identify the main

*Correspondence: C. Manfrin, Department of Life Sciences, University of Trieste, via L. Giorgieri 5, Trieste 34127, Italy. Tel: +39 040 558 8715. Fax: +39 040 575079. Email: cmanfrin@units.it

© 2018 The Author(s). Published by Informa UK Limited, trading as Taylor & Francis Group.
This is an Open Access article distributed under the terms of the Creative Commons Attribution License (http://creativecommons.org/licenses/by/4.0/), which permits unrestricted use, distribution, and reproduction in any medium, provided the original work is properly cited.

Published online 22 Jan 2018

phagocyting haemocyte after *in vivo* artificial non-self challenge with latex beads; (2) total and differential haemocyte counts; and (3) activity of basal and total phenoloxidase as a component of the humoral defence.

Invertebrates rely on innate defence mechanisms, involving cellular and humoral responses, for the recognition of invaders and their immobilisation. Three classes of haemocytes have been commonly described in crustaceans, including hyaline (HH), semigranular (SH) and granular haemocytes (GH) (Martin & Graves 1985; Hose et al. 1990; Johansson et al. 2000; Battison et al. 2003; Ding et al. 2012). In the crayfish (*Pontastacus*) *leptodactylus*, ultrastructural features allowed the characterisation of a fourth class of haemocytes containing granules with an intermediate diameter with respect to those of SH and GH (Giulianini et al. 2007). These different classes of haemocytes perform a series of coordinated activities integrating cellular and humoral responses, such as phagocytosis, encapsulation, early non-self recognition, melanisation, coagulation, prophenoloxidase-activating system, antimicrobial peptides and cytotoxicity (Martin & Graves 1985; Hose et al. 1990; Johansson et al. 2000; Battison et al. 2003; Vazquez et al. 2009; Lin & Soderhall 2011). Humoral defences include the production of antimicrobial peptides (AMPs), reactive intermediates of oxygen or nitrogen, and the prophenoloxidase enzymatic cascade (proPO) regulating melanisation of haemolymph (Yang et al. 2013).

In the present work, we compared the immune parameters measured in a control group with those of red swamp crayfish irradiated with a dose of 40 Gy to evaluate the effects of X-rays on the immune response of this species.

Material and methods

Animal collection and housing conditions

Adult crayfish (40.7 ± 0.5 mm, n = 70) were collected in April–July 2014 from Casette Lake (Pordenone, Friuli Venezia Giulia, Italy) during the reproductive season. Once in the laboratory, they were kept at a density of 15 ind./m^2 in plastic tanks (80 × 60 × 60 cm) containing 48 L of tap water and halved terracotta pots as shelters. For the entire period of the study, experimental individuals were maintained under a 12:12 h light/dark cycle, at room temperature (20°C) and fed *ad libitum* with crayfish pellets (Sera granular, Heisenberg, Germany). Water was changed twice a week.

The experiments comply with the current laws of Italy, the country in which they were done. No specific permits are required for studies that do not involve endangered or protected species. Individuals were maintained in appropriate laboratory conditions to guarantee their welfare and responsiveness. After the experiments were completed, crayfish were sacrificed by hypothermia.

Irradiation of males

Twenty males were irradiated with a dose of 40 Gy in accordance with Piazza et al. (2015). The irradiation was carried out on 12 August 2016 at the Pordenone Hospital (Pordenone, Italy). During the irradiation, crayfish were maintained in a plastic tank (17 × 29 × 36 cm) with 10 L of tap water and covered with a sheet of Plexiglas (thickness: 2 cm). A clinical linear accelerator (Siemens Mevatron MX2) with a 4-MeV electron beam was used to generate X-rays yielding 2 Gy/min at 100 cm from the target (40 × 30 cm), so that the treatment doses were achieved with 20 min of exposure. After the treatment, crayfish were kept isolated for 2 weeks in individual aquaria (25 × 20 × 20 cm), each containing a shelter (a halved terracotta pot), and were observed daily to assess possible alterations in their general activity. Twenty males were subjected to the same manipulation, but not irradiated, serving as the control group. The haemolymph was collected 20 days after the irradiation for ultrastructural and enzymatic analyses. Twenty days represents an intermediate time point between 10 days after irradiation, where initial structural damages were noticed, and 30 days after irradiation, where extended cellular and structural damage was observed (Piazza et al. 2015).

In vivo phagocytosis assay

To assess the ability of crayfish haemocytes to phagocytise foreign material, we used a 26-gauge needle to inject 100 µL of carboxylate-modified polystyrene latex beads (0.9 µm in diameter, aqueous suspension, 10% solids content, Sigma) diluted 1:1 in 0.15 M sterile phosphate buffered saline (PBS, Sigma) into the pericardial sinus of the crayfish (LB group). A second group was injected with 100 µL of sterile PBS (PBS group). Untreated animals were used as the control (CTRL group). After 2 h, 200 µL of haemolymph was withdrawn from the pericardial sinus of each animal into a sterile plastic 1-mL syringe (26-gauge needle), filled with an equal volume of fixative (2.5% glutaraldehyde, 0.8% paraformaldehyde and 7.5% saturated aqueous solution of picric acid in 0.15 M PBS, pH 7.4, with 1.5% sucrose). After a fixation of 10 min, haemocytes were pelleted in 1 mL of fixative by 14,000 rpm centrifugation for 10 min at 20°C. The resulting pellets were

then washed in 0.15 M PBS, pH 7.4, and post-fixed in 1% osmium tetroxide in the same buffer, serially dehydrated in ethanol and embedded, via propylene oxide, in Embed812/Araldite (Electron Microscopy Sciences, Fort Washington, PA).

For transmission electron microscopy, ultra-thin sections (120 nm) were cut with a Leica Ultracut UTC Ultratome, stained with uranyl acetate and lead citrate, and examined with a Philips EM 208 electron microscope at 100 kV; images were acquired with a Quemesa bottom-mounted TEM CCD Camera (Olympus, Germany) provided with an iTEM imaging platform and saved in TIF format.

For light microscopy, semi-thin sections (2 μm) were stained with toluidine blue and examined with an Olympus BX50; images were acquired with a digital Olympus E-P1 camera. The analysis of the images was performed with the open-source program ImageJ 1.50i (Schneider et al. 2012). Circularity of haemocytes granules was calculated with the same ImageJ shape descriptor where a circularity value of 1.0 indicates a perfect circle. As the value approaches 0.0, it indicates an increasingly elongated polygon.

Haemocyte counts

Total and differential haemocyte counts were performed for specimens from CTRL, PBS, LB and irradiated groups. For total haemocyte counts (THCs), 50 μL of haemolymph was collected from each animal and haemocytes were counted using a Bürker's haemocytometer. For differential haemocyte counts (DHCs), haemolymph was processed as described above for light and electron microscopy. Three differential cell counts were made by two different operators from semi-thin (2 μm) transverse sections of the full pellet thickness stained with toluidine blue. From 88 to 601 haemocytes were scored from three slides per pellet. Neither aggregate latex beads nor aggregate cells were found in the pellets. Cells with ambiguous features were scored as not classified (NC).

Basal and total plasmatic phenoloxidase activities

Haemolymph withdrawal was performed through the abdominal haemolymph sinuses. Plasma was isolated from haemocytes through centrifugation. Phenoloxidase (PO) activity was monitored spectrophotometrically as the formation of dopachrome from 3, 4-dihydroxy-L-phenylalanine (L-DOPA, Sigma-Aldrich). For the determination of basal PO, 20 μL of plasma was taken and mixed with 180 μL of L-DOPA (3 mg/mL in PBS) in a microtiter plate. For the determination of total plasmatic PO (pPO) enzyme activity, 30 μL of plasma was added to 30 μL of methanol that chemically activates PO from its inactive zymogen, prophenoloxidase (proPO) (Yang et al. 2013). The haemolymph–methanol mixture was incubated for 5 min at room temperature and 20 μL was mixed with 180 μL of L-DOPA (3 mg/mL in PBS) in a microtiter plate. The basal and total phenoloxidase enzyme activity at 20°C was recorded at 492 nm for 30 min at 5-min intervals using a plate reader (Sirio S, SEAC). All samples were assayed in duplicate. The enzyme activity was measured as the slope (absorbance vs time) of the reaction curve during the linear phase of the reaction. The slope of the reaction curve at V_{max} was plotted as absorbance per μL of haemolymph per min. PO assay was performed for CTRL (n = 11), LB (n = 9), and irradiated (n = 10) groups.

Statistical analysis

Statistical analyses were performed using R version 3.4.1 software (R Core Team 2016). Differences among the experimental groups in haemolymph plasmatic PO activity, THCs, DHCs and granule shape descriptors were assessed by nonparametric statistics, i.e. Kruskal–Wallis rank sum test followed by post-hoc Wilcoxon rank sum test pairwise comparisons with Bonferroni correction, since the null hypothesis of the Bartlett test for the homogeneity of variance could not be rejected. The box-and-whiskers plots were drawn with the boxplot command. All values are reported as mean ± standard error (SE) in the text. Differences were considered significant at p-value ≤ 0.05.

Results

Haemocyte types and morphology

Three morphological types of circulating cells were identified in sections of fixed pellet by transmission electron microscopy: hyaline haemocytes (HH; Figures 1(a), and 4(a)), semigranular haemocytes (SH; Figures 1(c), 2(a,b) and 4(b)) and granular haemocytes (GH; Figures 1(d–f) and 4(c)).

HHs are the smallest circulating haemocytes, with an oval/irregular profile (Figure 1(a,b)), high nucleus/cell surface ratio and a mean diameter of 9.89 ± 0.65 μm (n = 10).

The nucleus, euchromatic and sometimes lobated, is located in a central position and presents large chromatin lumps. In the cytoplasm, rough endoplasmic reticulum, mitochondria and small electron-dense vesicles with a mean diameter of 0.35 ± 0.02 μm (n = 20) are present (Figure 4(a)).

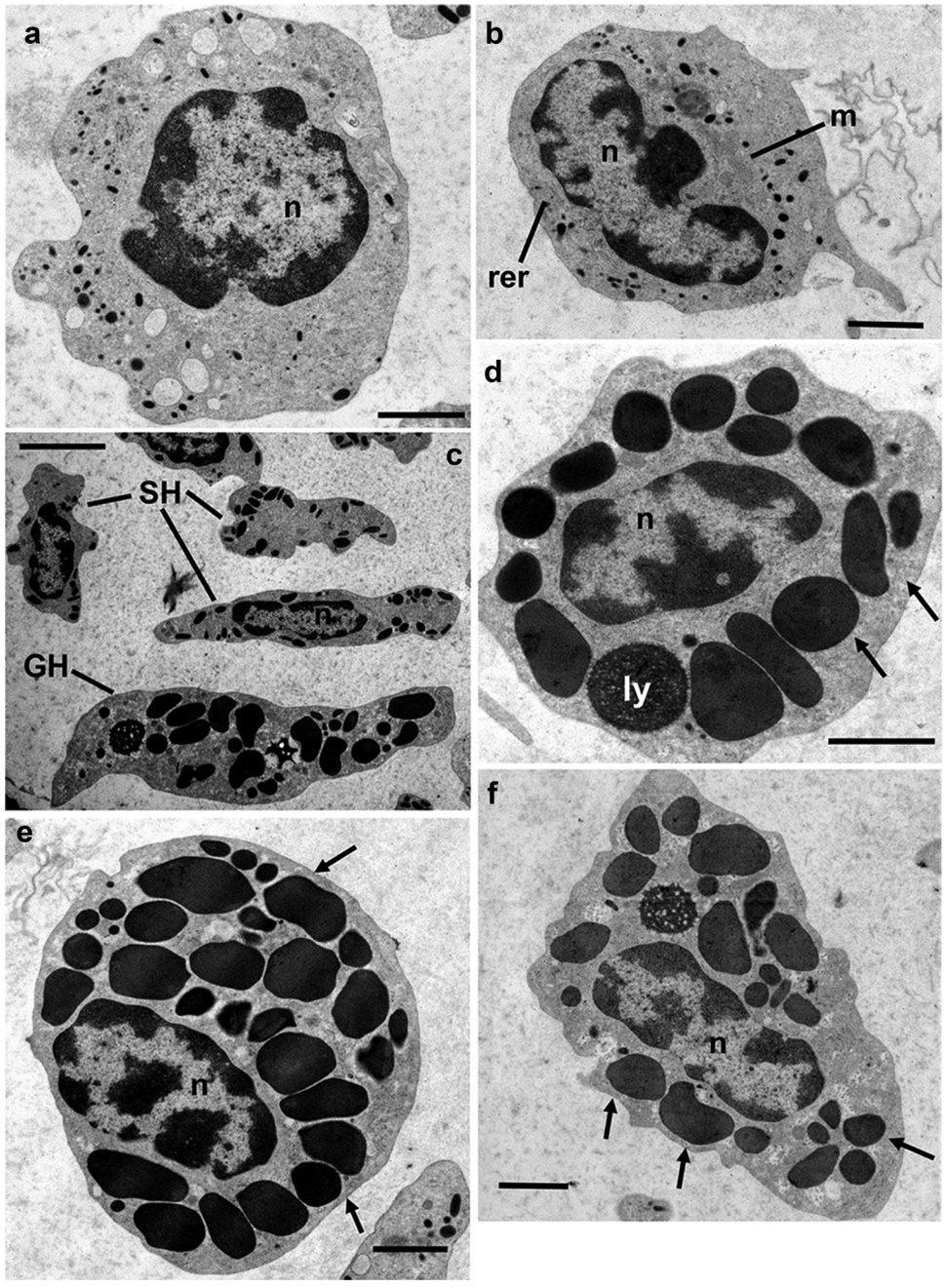

Figure 1. Transmission electron microscopy of *Procambarus clarkii* haemocytes, CTRL group. (a,b) Hyaline haemocytes (HH) showing a high nucleus/cell ratio. (c) Granular (GH) and semigranular haemocytes (SH). Transversal (d,e) and longitudinal (f) section of granular haemocytes (GH). Arrows: granules; ly: lysosome; m: mithocondria; n: nucleus; rer: rough endoplasmic reticulum. Scale bars: a, b, d–f = 2 μm; c = 5 μm.

SHs present an elongated profile of 12.38 ± 0.92 μm in length and 6.22 ± 0.30 μm in width (n = 10) (Figures 1(c) and 2(a, b)).

The large nucleus is located in a central position with an irregular, sometimes lobated and polymorphic profile. The cytoplasm presents a well-developed rough endoplasmic reticulum, Golgi complex and elongated mitochondria with tabular cristae (Figure 2(b)). Homogeneous electro-dense granules with a mean diameter of 0.74 ± 0.03 μm (n = 20) are present (Figure 3(a)).

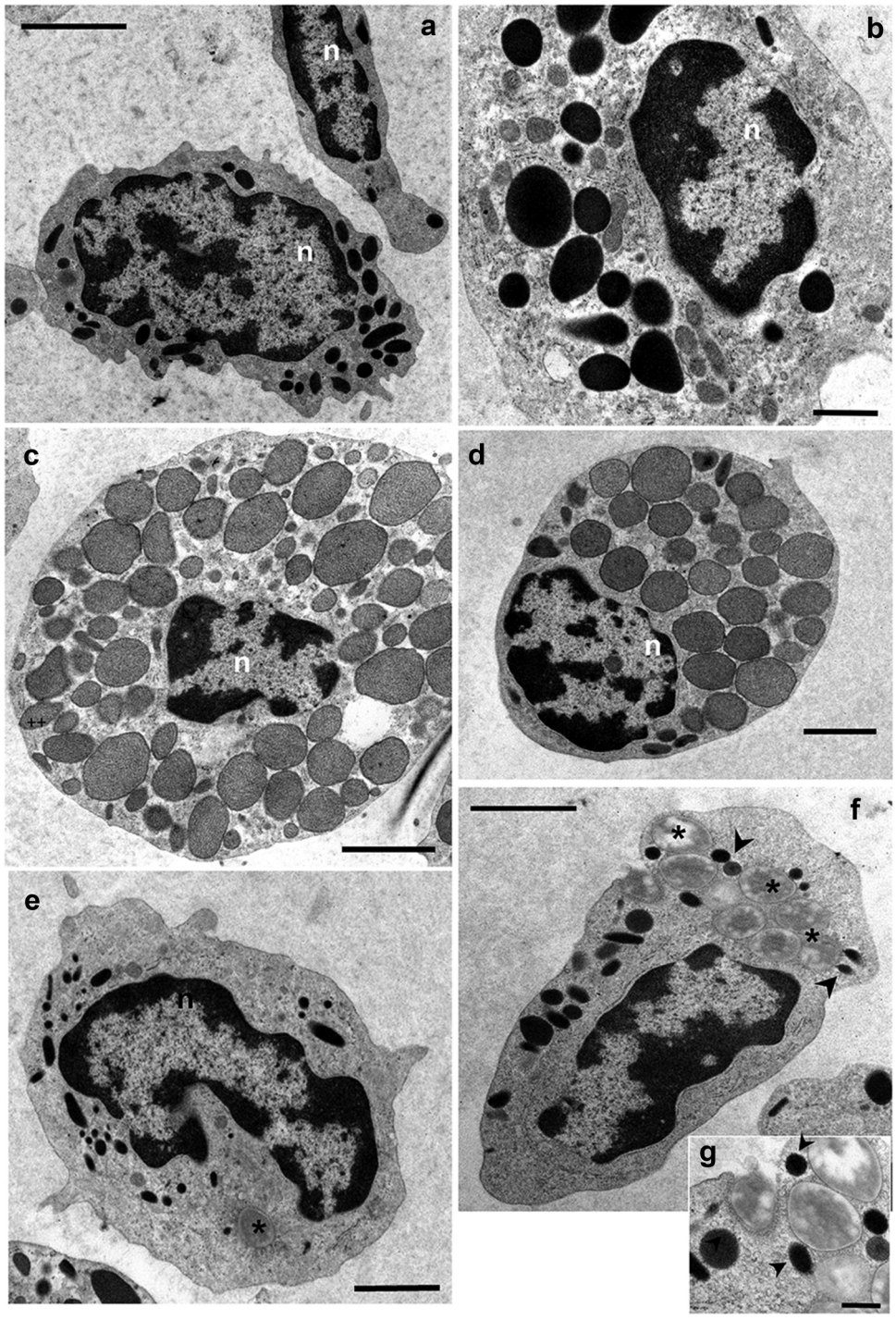

Figure 2. Transmission electron microscopy of *Procambarus clarkii* haemocytes, latex beads group. (a,b) semigranular haemocyte (SH). (c,d) medium granules haemocyte (MH). (e,f) Semigranular haemocyte (SH) involved in phagocytic activity after *in vivo* artificial non-self-challenge. A large number of latex beads (asterisks) are present in the cytoplasm included into the phagosomes. (g) Detail of semigranular haemocytes (SHs) showing the latex bead phagocytosis at the membrane level. Many granules appear to be fusing with phagosomes (arrowheads). n: nucleus. Scale bars: b = 1 μm; a, c–f = 2 μm; g = 500 nm.

GHs present a circular to spindle-shaped profile with a mean diameter of 12.24 ± 0.81 μm (n = 10). The nucleoplasm is finely dispersed with some chromatin lumps mainly located

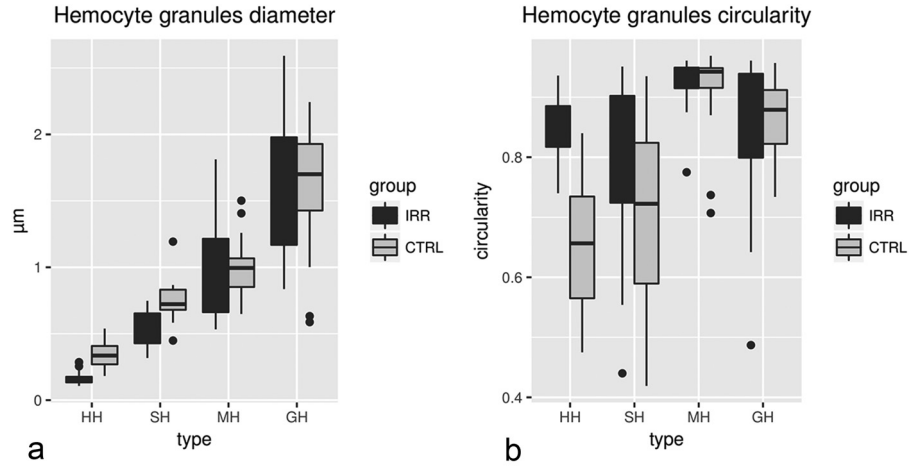

Figure 3. Diameter (a) and circularity (b) of granules characterising the four types of haemocytes. CTRL: control group, HH: Hyaline haemocytes, SH: semigranular haemocytes, MH: medium granule haemocytes, GH: granular haemocytes. IRR: irradiated group.

beneath the nuclear envelope. In the cytoplasm, some late endosomes are present. These haemocytes are characterised by large, electron-dense, amorphous, membrane-enclosed granules showing a round to oval or lentil-like granule profile with a mean diameter of 1.57 ± 0.09 µm (n = 20; Figure 3(a)).

Measures of granule diameters have highlighted a fourth type of haemocytes not detectable in traditional unfixed preparations observed with Nomarsky's contrast, while it is easily appreciable in ultrathin sections of pelleted haemocytes (Figures 2(d) and 4(c,d)). This medium granule haemocyte (MH) has variable electron-dense structured granules with a round profile and a mean diameter of 0.99 ± 0.05 µm (n = 20) in the cytoplasm, that is significantly different that of the granules of other haemocyte types (Wilcoxon rank sum test, $p \leq 0.003$; Figure 3(a)). The MHs have a round profile, about 13.16 ± 0.96 µm (n = 10) in diameter. The euchromatic nucleus, mainly located in an eccentric position, presents a circular/irregular profile. The circular function highlights that structured granules of MH exhibit the significantly greatest circularity compared to granules of other haemocyte categories (0.91 ± 0.16, n = 20; Wilcoxon rank sum test, $p \leq 0.0107$; Figure 3(b)). MH from an irradiated male exhibits both typical structured granules and large, electron-dense, structureless, GH-like granules (Figure 4(e)).

Circulating haemocytes of males irradiated with a dose of 40 Gy show significantly lower diameters in the granules of HH and SH in comparison with diameters of granules of the same haemocyte types of un-irradiated males (0.17 ± 0.01, n = 20 and 0.52 ± 0.03, n = 20; Wilcoxon rank sum test, $p \leq 0.0001$; Figure 3). The granules of HH exhibit a significantly greater circularity (0.85 ± 0.01, n = 20) in comparison with HH granules of un-irradiated males (0.65 ± 0.02, n = 20 and 0.52 ± 0.03, n = 20; Wilcoxon rank sum test, p = 3.92e-07; Figure 3). No other evident ultrastructural damages in comparison with un-irradiated animals were found (Figure 4(a–d)).

Haemocyte phagocytic responses

SHs were able to phagocytise latex beads 2 h after the injection (Figure 2(e–g)). We observed these haemocytes with up to 10 phagocytised beads within the cytoplasm. Electro-dense granules fusing with a phagosome are evident, demonstrating their role as primary lysosomes (Figure 2(g)).

Total and differential haemocyte counts

The THCs in CTRL, PBS, LB and irradiated males (IRR) of *P. clarkii* are shown in Figure 5. In the Irradiated animals, THCs are highly significantly lower (432,857 ± 56,049 haemocytes/mL, n = 7) in comparison with CTRL (2,000,454 ± 235,640 haemocytes/mL, n = 11; Wilcoxon rank sum test, p = 0.003) and the PBS-injected group (1,006,071 ± 184,413 haemocytes/mL, n = 7; Wilcoxon rank sum test, p = 0.013), but not with LB-challenged ones (1,105,312 ± 296,687 haemocytes/mL, n = 8; Wilcoxon rank sum test, p = 0.251; Figure 5). No significant differences were recorded in the other pairwise comparisons (Wilcoxon rank sum test, $p > 0.07$).

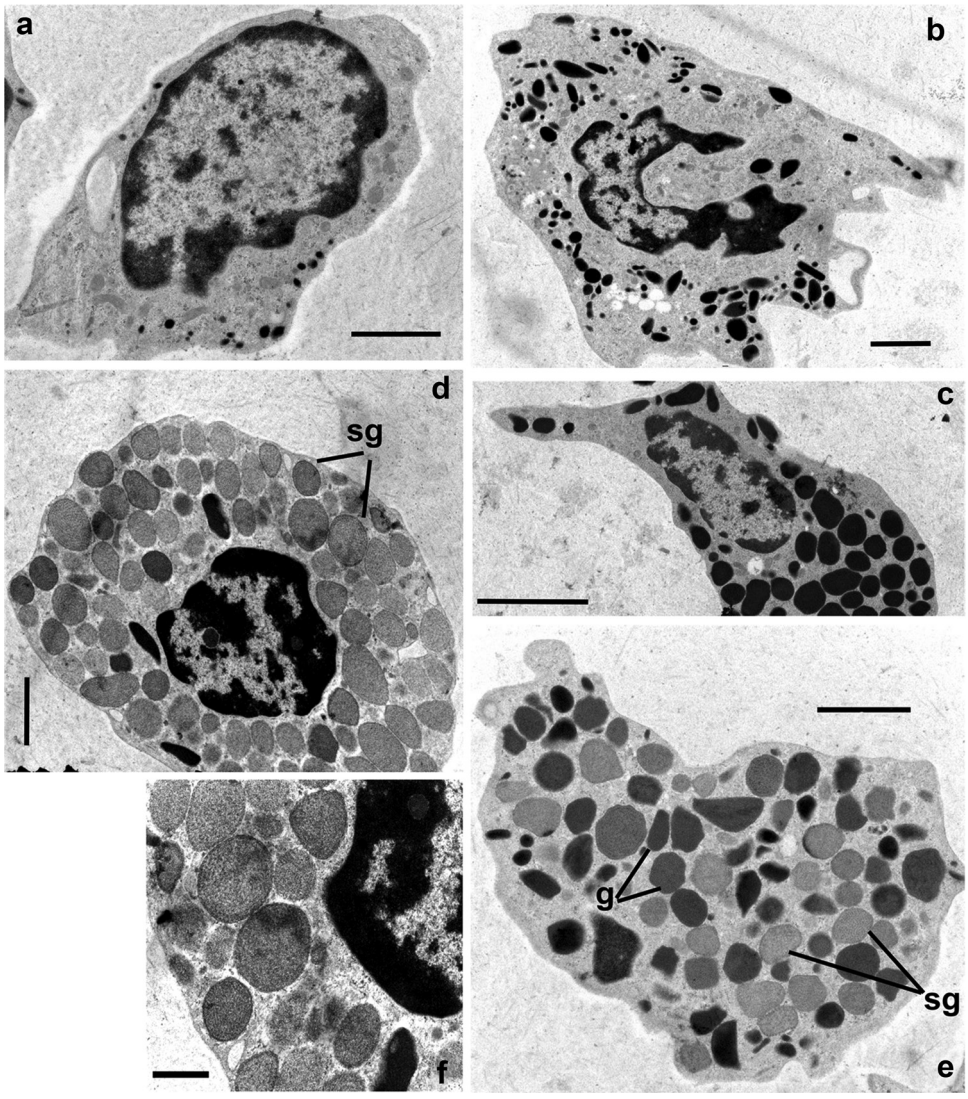

Figure 4. Transmission electron microscopy of *Procambarus clarkii* haemocytes 20 days after irradiation at a dose of 40 Gy. (a) Hyaline haemocytes: HH, Hyaline haemocyte. (b) Semigranular haemocytes: SH, Semigranular haemocyte. (c) Granular haemocytes: GH, Granular haemocyte. (d,e) Medium granule haemocytes: MH. (f) Detail of structured granules in MH, Medium granule haemocyte. (g) GH-like granules, sg: structured granules. Scale bars: f = 1 μm; a, b, d, e = 2 μm; c = 5 μm.

The DHCs show that HHs are the main haemocyte type in haemolymph of CTRL (59.7 ± 4.9, n = 9), PBS (65.8 ± 2.7, n = 6) and LB groups (67.6 ± 4.0, n = 6) (Figure 6). Significantly lower HH percentages are recorded in the IRR group (17.6 ± 5.2, n = 10) compared with CTRL (Wilcoxon rank sum test, p = 0.0048), PBS (Wilcoxon rank sum test, p = 0.0119) and LB (Wilcoxon rank sum test, p = 0.0119). SH percentages are significantly higher in IRR (25.5 ± 5.0, n = 10), in CTRL (13.2 ± 3.0, n = 9) and in PBS (9.9 ± 0.8, n = 6) compared to LB (5.5 ± 0.8, n = 6; Wilcoxon rank sum test, p = 010 and p = 0.046). The irradiated group shows significantly higher GH percentages (48.6 ± 6.2, n = 10) in comparison with CTRL (18.0 ± 2.1, n = 9; Wilcoxon rank sum test, p = 0.0065), PBS (20.9 ± 3.2, n = 6; Wilcoxon rank sum test, p = 0.04) and LB (21.9 ± 3.4, n = 6; Wilcoxon rank sum test, p = 0.028). NC cells do not present significant differences among groups (Wilcoxon rank sum test, $p \geq 0.30$).

Phenoloxidase (PO) activity

The results show no significant differences in basal PO and total plasmatic PO activities among CTRL, LB and IRR groups of *P. clarkii* males (Wilcoxon rank sum test, $p \geq 0.05$; Figure 7).

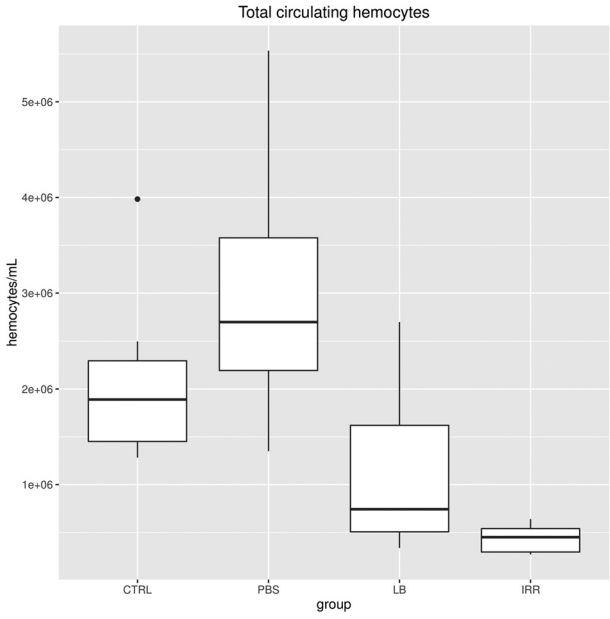

Figure 5. Total circulating haemocytes from control (CTRL), PBS group (PBS), latex beads (LB) and irradiated (IRR) groups.

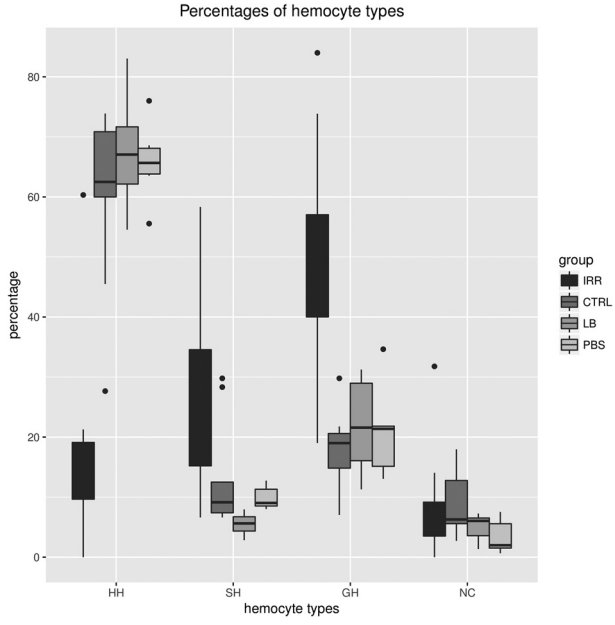

Figure 6. Differential haemocyte percentages in *Procambarus clarkii* male from control (CTRL), PBS group (PBS), latex beads (LB) and irradiated (IRR) groups.

Discussion

In the present study three major types of circulating haemocytes were identified by transmission electron microscopy: HHs, SHs and GHs. The ultrastructural features of *P. clarkii* haemocytes agree with those already described for SH and GH. As regards HH,

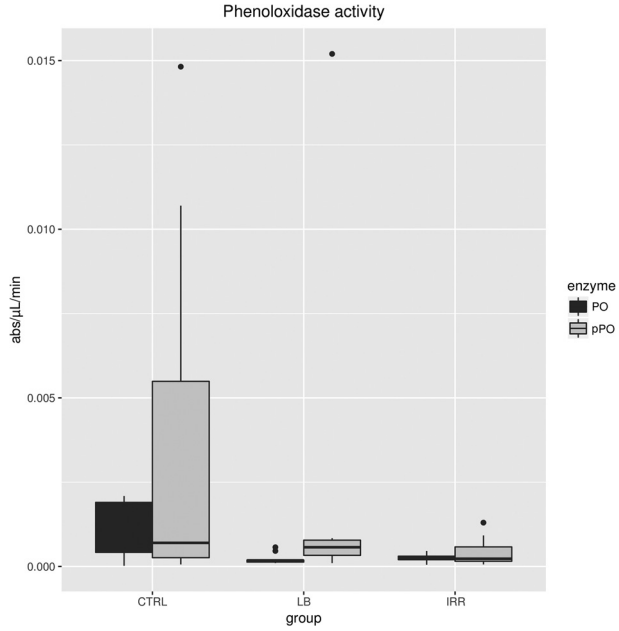

Figure 7. Basal (PO) and total plasmatic phenoloxidase (pPO) activities in *Procambarus clarkii* males from control (CTRL), latex beads (LB) and irradiated (IRR) groups measured as the slope of the reaction curve at V_{max}. The enzymatic activities were recorded as absorbance units for µL of haemolymph per min (for statistics see the text).

Ding and colleagues (2012) described HHs with no granules, but this was not observed in haemocyte pellets from this study. Moreover, the ultrastructural features of haemocyte granules allowed the characterisation of a fourth type of haemocyte, MH, with electron-dense inhomogeneous granules with a round profile and a mean diameter of 0.99 ± 0.05 µm, and showing intermediate dimensions compared to granules of SH and GH. This type of haemocyte was already described in the crayfish *Astacus leptodactylus* (Giulianini et al. 2007). Due to the difficulties of recognising this haemocyte type at light microscopy level, MHs were not counted for the DHCs and probably fell into the NC category. The occurrence of an MH containing also GH-like granules suggests that this haemocyte represents an immature stage of the GH. The differences in the observed percentages of haemocyte types of a previous study on the same species (Ding et al. 2012) depend on (1) the different categorisation of the haemocytes and (2) the different methodology used for their characterisation, since we counted them in semi-thin stained sections unlike the cited authors who distinguished them by means of phase contrast or bright-field light microscopy. For instance, the high percentages of HHs of the present work (59.7 ± 4.9) are more in accordance with those recorded by the same methodology in *A. leptodactylus*

(46.7 ± 4.9), rather than with those recorded in *P. clarkii* with a different technique (16.3 ± 2.2; Giulianini et al. 2007; Ding et al. 2012). Besides, the present study identifies the SH as the haemocyte type primarily involved in phagocytic activity after *in vivo* artificial non-self challenge with latex beads, in accordance with what was already described for *A. leptodactylus* (Giulianini et al. 2007).

The literature documents a survival of males irradiated with a dose of 20 Gy, reared under laboratory conditions, of at least 1 year (Aquiloni et al. 2009). In the present study, only one male out of 20 died during the experiment, indicating the very low mortality rate of this species after X-ray irradiation of 40 Gy. The selected time point of 20 days represents an intermediate point between 10 days after the irradiation, where initial structural damage was noticed, and 30 days after radiation, where extended cellular and structural damage has been observed (Piazza et al. 2015).

We found a significant decrease of about 80% of circulating haemocytes and an increase in percentage of SH and GH in males irradiated with a dose of 40 Gy after 20 days. The considerable decrease in circulating haemocytes is consistent with the cytological damage to the gonads that was described as progressive from the day of irradiation up to 30 days (Piazza et al. 2015). As pointed out by some authors, in malacostracans the occurrence of circulating haemocytes in division is an exceptional phenomenon and it reflects the release, in the circulation, of immature haemocytes or prohaemocytes from haematopoietic sites (Bauchau 1981; Roulston & Smith 2011). The lack of noticeable ultrastructural damage induced by X-ray irradiation on circulating haemocytes is consistent with the finding that SH and GH are differentiated haemocytes whilst HH are pro-stages for the two above haemocyte lineages, as reported for *Penaeus monodon* (Van De Braak et al. 2002) and for *Pacifastacus leniusculus* (Wu et al. 2008; Söderhäll 2016). In *A. leptodactylus* ultrastructural features suggest that HH is a relatively undifferentiated haemocyte type whilst SH ("small granule haemocytes") and GH ("large granule containing haemocytes") show features of well-differentiated haemocyte types (Giulianini et al. 2007). The DHCs of the present study demonstrate that in the contest of a drastic reduction of total haemocytes in irradiated animals, the percentages of SHs and GHs significantly increase, in view of a collapse of the HH percentages that normally represent the highest percentages of circulating haemocytes, with means of more than 50%. This finding could be explained by (1) the damaged hematopoietic tissues not able to release new HH after irradiation and (2) the former HH, at the time of irradiation, progressively differentiating in the SH and GH types. The fact that most of the males show an apparently normal reactivity after 20 days of irradiation could be explained by cellular protective mechanisms that compensate for cell loss. In fact, with a dose of 4000 Roentgen (equivalent to 35.08 Gy), 60–75% of imaginal disc cells of *Drosophila melanogaster* third-instar larvae died, but the resulting adult flies were indistinguishable in size from un-irradiated controls, indicating a replacement of dead cells (Jaklevic & Su 2004). Interestingly, the activity of PO and pPO is not affected by ionising radiation after 20 days of the treatment, and this could, in part, explain the good survivorship of irradiated males that are able to face immunological challenges by humoral activity. In a recent study on the lepidopteran pest *Spodoptera litura*, it was reported that radioresistance increased in relation to the age of the insect (Sachdev et al. 2017), and the use of adult crayfish could explain the unaltered PO and pPO pathways. It remains to be seen how, and how long, animals are able to offset the drastic haemocyte decline, and whether this would preclude survival in the wild.

Acknowledgements

The authors are grateful to Dr Paolo Bertoncin (Servizio di Microscopia Elettronica, Università di Trieste) for his helpful suggestions and skilful technical support.

Funding

No funds to be declared [0000].

ORCID

C. Manfrin http://orcid.org/0000-0002-4979-8557

References

Aquiloni L, Becciolini A, Berti R, Porciani S, Trunfio C, Gherardi F. 2009. Managing invasive crayfish: Use of X-ray sterilisation of males. Freshwater Biology 54:1510–1519. DOI:10.1111/j.1365-2427.2009.02169.x.

Aquiloni L, Gherardi F. 2010. The use of sex pheromones for the control of invasive populations of the crayfish *Procambarus clarkii*: A field study. Hydrobiologia 649:249–254. DOI:10.1007/s10750-010-0253-4.

Battison A, Cawthorn R, Horney B. 2003. Classification of *Homarus americanus* hemocytes and the use of differential hemocyte counts in lobsters infected with *Aerococcus viridans var. homari* (Gaffkemia). Journal of Invertebrate Pathology 84:177–197. DOI:10.1016/j.jip.2003.11.005.

Bauchau AG. 1981. Crustaceans. In: Ratcliffe NA, Rowley AF, editors. Invertebrate blood cells. Vol. 2. New York: Academic Press. pp. 385–420.

Ding Z, Du J, Ou J, Li W, Wu T, Xiu Y, Meng Q, Ren Q, Gu W, Xue H, Tang J, Wang W. 2012. Classification of circulating hemocytes from the red swamp crayfish *Procambarus clarkii* and their susceptibility to the novel pathogen *Spiroplasma eriocheiris in vitro*. Aquaculture 356–357:371–380. DOI:10.1016/j.aquaculture.2012.04.042.

Giulianini PG, Bierti M, Lorenzon S, Battistella S, Ferrero EA. 2007. Ultrastructural and functional characterization of circulating hemocytes from the freshwater crayfish *Astacus leptodactylus*: Cell types and their role after in vivo artificial non-self challenge. Micron 38:49–57. DOI:10.1016/j.micron.2006.03.019.

Hose JE, Martin GG, Gerard AS. 1990. A Decapod hemocyte classification scheme integrating morphology, cytochemistry, and function. The Biological Bulletin 178:33–45. DOI:10.2307/1541535.

Jaklevic BR, Su TT. 2004. Relative contribution of DNA repair, cell cycle checkpoints, and cell death to survival after DNA damage in *Drosophila* larvae. Current Biology 14:23–32. DOI:10.1016/j.cub.2003.12.032.

Johansson MW, Keyser P, Sritunyalucksana K, Söderhäll K. 2000. Crustacean haemocytes and haematopoiesis. Aquaculture 191:45–52. DOI:10.1016/S0044-8486(00)00418-X.

Lin X, Soderhall I. 2011. Crustacean hematopoiesis and the astakine cytokines. Blood 117:6417–6424. DOI:10.1182/blood-2010-11-320614.

Martin GG, Graves BL. 1985. Fine structure and classification of shrimp hemocytes. Journal of Morphology 185:339–348. DOI:10.1002/jmor.1051850306.

Peruzza L, Piazza F, Manfrin C, Bonzi L, Battistella S, Giulianini P. 2015. Reproductive plasticity of a *Procambarus clarkii* population living 10°C below its thermal optimum. Aquatic Invasions 10:199–208. DOI:10.3391/ai.2015.10.2.08.

Piazza F, Aquiloni L, Peruzza L, Manfrin C, Simi S, Marson L, Edomi P. 2015. Managing of *Procambarus clarkii* by X-ray sterilisation of males: Cytological damage to gonads. Micron 77:32–40. DOI:10.1016/j.micron.2015.05.016.

R Core Team. 2016. R: A language and environment for statistical computing. Vienna, Austria: R Foundation for Statistical Computing.

Roulston C, Smith VJ. 2011. Isolation and in vitro characterisation of prohaemocytes from the spider crab, *Hyas araneus* (L.). Developmental & Comparative Immunology 35:537–544. DOI:10.1016/j.dci.2010.12.012.

Sachdev B, Khan Z, Zarin M, Malhotra P, Seth RK, Bhatnagar RK. 2017. Irradiation influence on the phenoloxidase pathway and an anti-oxidant defense mechanism in *Spodoptera litura* (Lepidoptera: Noctuidae) and its implication in radio-genetic 'F_1 sterility' and biorational pest suppression tactics. Bulletin of Entomological Research 107:281–293. DOI:10.1017/S0007485316000961.

Schneider CA, Rasband WS, Eliceiri KW. 2012. NIH Image to ImageJ: 25 years of image analysis. Nature Methods 9:671–675. DOI:10.1038/nmeth.2089.

Söderhäll I. 2016. Crustacean hematopoiesis. Developmental & Comparative Immunology 58:129–141. DOI:10.1016/j.dci.2015.12.009.

Souty-Grosset C, Anastácio PM, Aquiloni L, Banha F, Choquer J, Chucholl C, Tricarico E. 2016. The red swamp crayfish *Procambarus clarkii* in Europe: Impacts on aquatic ecosystems and human well-being. Limnologica - Ecology and Management of Inland Waters 58:78–93. DOI:10.1016/j.limno.2016.03.003.

Van de Braak CB, Botterblom MHA, Huisman EA, Rombout J, Van Der Knaap WP. 2002. Preliminary study on haemocyte response to white spot syndrome virus infection in black tiger shrimp, *Penaeus monodon*. Diseases of Aquatic Organisms 51:149–155. DOI:10.3354/dao051149.

Vazquez L, Alpuche J, Maldonado G, Agundis C, Pereyra-Morales A, Zenteno E. 2009. Review: Immunity mechanisms in crustaceans. Innate Immunity 15:179–188. DOI:10.1177/1753425909102876.

Wu C, Söderhäll I, Kim Y-A, Liu H, Söderhäll K. 2008. Hemocyte-lineage marker proteins in a crustacean, the freshwater crayfish, *Pacifastacus leniusculus*. Proteomics 8:4226–4235. DOI:10.1002/pmic.200800177.

Yang B, Lu A, Peng Q, Ling Q, Ling E. 2013. Activity of fusion prophenoloxidase-GFP and its potential applications for innate immunity study. PLoS ONE 8:e64106. DOI:10.1371/journal.pone.0064106.

Yazicioglu B, Reynolds J, Kozák P. 2016. Different aspects of reproduction strategies in crayfish: A review. Knowledge and Management of Aquatic Ecosystems 417:15. DOI:10.1051/kmae/2016020.